Nonlinear-optical spectral transformation of few-cycle laser pulses in photonic-crystal fibers

E. E. Serebryannikov,[1] A. M. Zheltikov,[1,*] N. Ishii,[2] C. Y. Teisset,[2] S. Köhler,[2] T. Fuji,[2] T. Metzger,[2] F. Krausz,[2,3] and A. Baltuška[2,†]

[1]*Physics Department, International Laser Center, M. V. Lomonosov Moscow State University, Vorob'evy gory, Moscow 119992, Russia*

[2]*Max-Planck-Institut für Quantenoptik, Hans-Kopfermann-Strasse 1, D-85748 Garching, Germany*

[3]*Department für Physik, Ludwig-Maximilians-Universität Munich, D-85748 Garching, Germany*

(Received 31 May 2005; published 4 November 2005)

Photonic-crystal fibers with special dispersion profiles are shown to provide a high efficiency of spectral transformation of chirped sub-6-fs Ti:sapphire laser pulses. With the wavelength of zero group-velocity dispersion of the fiber lying within the broad spectrum of the input few-cycle pulse, the output spectra feature well-resolved spectral peaks, indicative of soliton self-frequency shift, four-wave mixing, and Cherenkov emission of dispersive waves. We demonstrate that up to 3% of radiation energy at the output of the fiber can be confined within a spectrally isolated soliton peak centered at 1060 nm, which is ideally suited as a seed for Nd:YAG- and ytterbium-based laser devices.

DOI: 10.1103/PhysRevE.72.056603 PACS number(s): 42.65.Sf, 42.81.Qb, 42.65.Wi

I. INTRODUCTION

Frequency conversion of ultrashort laser pulses is an interesting and challenging problem of modern optical science. Few-cycle laser pulses attainable with modern laser systems [1,2] are represented by broad spectra in the frequency domain. Efficient nonlinear-optical transformation of such field waveforms requires careful engineering of dispersion profiles of nonlinear materials for broadband phase and group-velocity matching and an optimal balance between dispersion and nonlinearity. Photonic-crystal fibers (PCFs) [3,4] are giving a new momentum to this field, providing large interaction lengths [5], strong confinement of electromagnetic field in a small fiber core [6], and offering a unique flexibility in dispersion engineering [7].

Evolution of broadband field waveforms in PCFs has been extensively examined during the past few years in the context of supercontinuum generation [8,9]. These studies have revealed significant features in the spectral evolution of broadband field waveforms in PCFs related to self-phase modulation (SPM) [10,11], four-wave mixing (FWM) [12], stimulated Raman scattering [13], Cherenkov emission of dispersive waves by solitons [14,15], soliton self-frequency shift (SSFS) [16], and cross-phase modulation (XPM) [17,18]. Scenarios of nonlinear-optical transformations of laser pulses have been shown [19] to be sensitive to the detuning of the central frequency of the input pulse relative to the wavelength of zero group-velocity dispersion (GVD).

In the case considered in this work, the input field has the form of a few-cycle pulse, defining a broadband field waveform with a nonunfirom spectral phase already as the initial condition for the evolution problem. We will show that PCFs can provide a high efficiency of spectral transformation of such field waveforms through phase modulation and FWM processes, as well as soliton frequency shifting and Cherenkov-type dispersive-wave emission. With the wavelength of zero group-velocity dispersion of the fiber lying within the broad spectrum of the input pulse, the output spectra are dominated by distinct spectral peaks, originating from concurrent nonlinear-optical processes. We identify well-resolved signatures of soliton self-frequency shift, four-wave mixing, and Cherenkov emission of dispersive waves and demonstrate that the laser pulse energy can be efficiently coupled into a spectrally isolated soliton-shifted peak centered at 1060 nm.

II. MODELING

Our theoretical analysis of propagation of laser pulses in PCFs was based on the numerical solution of the generalized nonlinear Schrödinger equation [20],

$$\frac{\partial A}{\partial z} = i\sum_{k=2}^{6} \frac{(i)_k}{k!}\beta^{(k)}\frac{\partial^k A}{\partial \tau^k} + i\gamma\left(1+\frac{i}{\omega_0}\frac{\partial}{\partial \tau}\right) \times \left(A(\tau,z)\int_{-\infty}^{\infty} R(\eta)|A(z,\tau-\eta)|^2 d\eta\right), \quad (1)$$

where A is the field amplitude, $\beta^{(k)}=\partial^k\beta/\partial\omega^k$ are the coefficients in the Taylor-series expansion of the propagation constant β, ω_0 is the carrier frequency, τ is the retarded time, $\gamma=(n_2\omega_0)/(cS_{\mathrm{eff}})$ is the nonlinear coefficient, n_2 is the nonlinear refractive index of the PCF material, $S_{\mathrm{eff}}=[\int_{-\infty}^{\infty}\int_{-\infty}^{\infty}|F(x,y)|^2dxdy]^2/\int_{-\infty}^{\infty}\int_{-\infty}^{\infty}|F(x,y)|^4dxdy$ is the effective mode area [$F(x,y)$ is the transverse field profile in the PCF mode], and $R(t)$ is the retarded nonlinear-response function. For fused silica, we take $n_2\approx 3.2\times 10^{-16}$ cm^2/W, and the $R(t)$ function is represented in a standard form [21],

$$R(t) = (1-f_R)\delta(t) + f_R\Theta(t)\frac{\tau_1^2+\tau_2^2}{\tau_1\tau_2^2}e^{-t/\tau_2}\sin\left(\frac{t}{\tau_1}\right), \quad (2)$$

where $f_R=0.18$ is the fractional contribution of the Raman response; $\delta(t)$ and $\Theta(t)$ are the delta and the Heaviside step

*Email address: zheltikov@phys.msu.ru

†Email address: andrius.baltuska@mpq.mpg.de

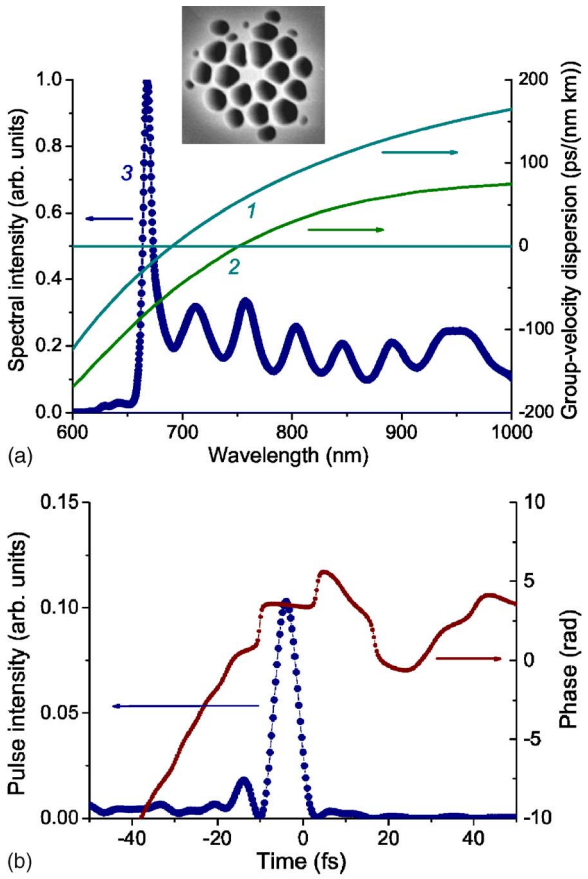

FIG. 1. (Color online) (a) Group-velocity dispersion as a function of the wavelength for the fundamental mode of (curve 1) the fused silica photonic-crystal fiber with a core diameter of 1.6 μm (shown in the inset) and (curve 2) NL-PM-750 PCF from Crystal Fibre. Curve 3 shows the intensity spectrum of the input laser pulse (Ti:sapphire oscillator output). (b) Temporal envelope and chirp of the Ti:sapphire oscillator output reconstructed from SPIDER data.

functions, respectively; $\tau_1=12.5$ fs and $\tau_2=32$ fs are the characteristic times of the Raman response of fused silica.

We now apply Eqs. (1) and (2) to compute the evolution of ultrashort pulses in two types of PCFs used in our experiments. PCFs of the first type consist of a fused silica core with a diameter of 1.6 μm, surrounded with two cycles of air holes [inset in Fig. 1(a)]. To find parameters $\beta^{(k)}$ for these fibers, we numerically solved the Maxwell equations for the transverse components of the electric field in the cross section of a PCF using a modification of the method of polynomial expansion in localized functions, developed by Monro *et al.* [22]. Polynomial approximation of the frequency dependence of the propagation constant β for the fundamental mode of the PCF computed with the use of this numerical procedure with an accuracy better than 0.1% within the range of wavelengths from 580 to 1220 nm yields the following $\beta^{(k)}$ coefficients for the central wavelength of 800 nm: $\beta^{(2)} \approx -0.0293$ ps^2/m, $\beta^{(3)} \approx 9.316\times10^{-5}$ ps^3/m, $\beta^{(4)} \approx -9.666\times10^{-8}$ ps^4/m, $\beta^{(5)} \approx 1.63\times10^{-10}$ ps^5/m, and $\beta^{(6)} \approx -3.07\times10^{-13}$ ps^6/m. Curve 1 in Fig. 1(a) displays the group-velocity dispersion (GVD) $D=-2\pi c\lambda^{-2}\beta^{(2)}$, where λ is the radiation wavelength, for the fundamental mode of such PCFs as a function of the wavelength. The GVD vanishes at $\lambda_z \approx 690$ nm. Fibers of the second type are commercial NL-PM-750 PCFs from Crystal Fibre [23]. The core diameter for these PCFs was equal to 1.8 μm. Parameters $\beta^{(k)}$ for these PCFs were defined as polynomial expansion coefficients for the dispersion profile of the fundamental mode of these fibers provided by the manufacturer [23]. The group-velocity dispersion for PCFs of this type is presented by curve 2 in Fig. 1(a). In this case, the GVD vanishes at $\lambda_z \approx 750$ nm.

In the case studied here, the laser field at the input of a PCF has a form of a few-cycle pulse [curve 1 in Fig. 1(b)] with a broad spectrum [curve 3 in Fig. 1(a)] and a complex chirp [curve 2 in Fig. 1(b)]. For both types of PCFs used in our experiments, the short-wavelength part of the spectrum lies in the range of normal dispersion, while the wavelengths above λ_z experience anomalous dispersion. Typical scenarios of spectral and temporal evolution of a few-cycle laser pulse in PCFs of the considered types are illustrated by Figs. 2 and 3. The initial stage of nonlinear-optical transformation of a few-cycle pulse involves self-phase modulation, which can be viewed as four-wave mixing of different frequency components belonging to the broad spectrum of radiation propagating through the fiber. Frequency components lying near the zero-GVD wavelength of the PCF then serve, as shown in the classical texts on nonlinear fiber optics [20], as a pump for phase-matched FWM. Such phase-matched FWM processes, which involve both frequency-degenerate and frequency-nondegenerate pump photons, deplete the spectrum of radiation around the zero-GVD wavelength and transfer the radiation energy to the region of anomalous dispersion [spectral components around 920 nm for $z=2$ cm in Fig. 2(b) and around 930 nm for $z=5$ cm in Fig. 3(a)]. A part of this frequency-downconverted radiation then couples into a soliton, which undergoes continuous frequency downshifting due to the Raman effect [Figs. 2(b) and 3(a)], known as soliton self-frequency shift [20,24,25]. In the time domain, the redshifted solitonic part of the radiation field becomes delayed with respect to the rest of this field [Fig. 2(a) and the insets in Figs. 3(a) and 3(b)] because of the anomalous GVD of the fiber. As a result of these processes, the redshifted soliton becomes more and more isolated from the rest of the light field in both time and frequency domain, which reduces, in particular, the interference between the solitonic and nonsolitonic part of radiation, seen in Figs. 2(b), 3(a), and 3(b).

High-order fiber dispersion induces soliton instabilities, leading to the Cherenkov-type emission of dispersive waves [26,27] phase-matched with the soliton, as discussed in the extensive literature (see, e.g., [14,15]). This resonant dispersive-wave emission gives rise to a spectral band centered around 540 nm in Fig. 2(b). As a result of the above-described nonlinear-optical transformations, the spectrum of the radiation field for a PCF with a characteristic length of 20 cm typically features four isolated bands, representing the remainder of the FWM-converted pump field [the bands centered at 670 and 900 nm in Fig. 2(b)], the redshifted solitonic part [reaching 1.06 μm for $z=24$ cm in Fig. 2(b)], and the blueshifted band related to the Cherenkov emission of dispersive waves in the visible. In the time domain, as can be seen from Fig. 2(a) and the insets to Figs. 3(a) and 3(b), only

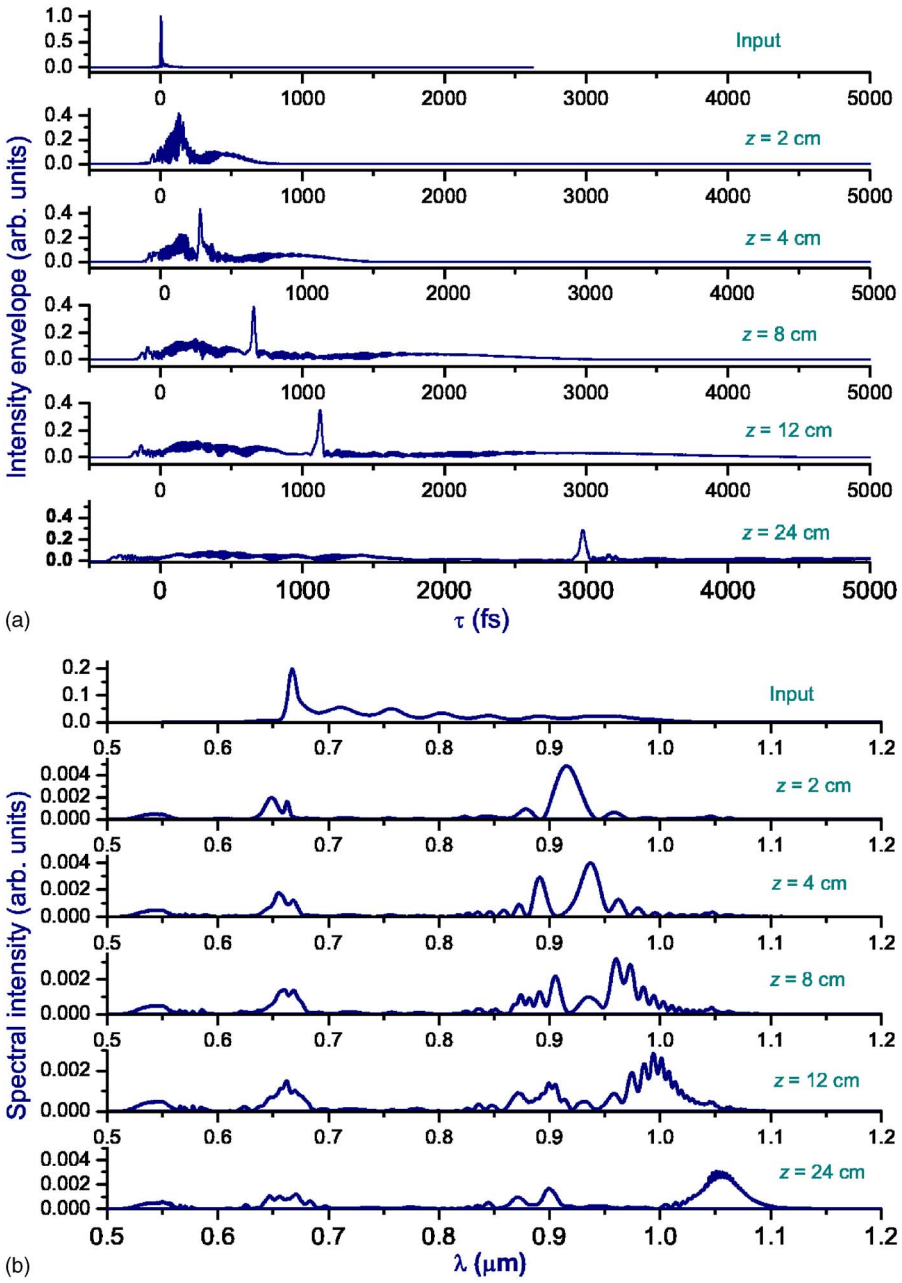

FIG. 2. (Color online) Temporal (a) and spectral (b) evolution of a laser pulse with an initial energy of 0.25 nJ and an input temporal envelope and chirp shown in Fig. 1(b) propagating through the PCF with the dispersion profile as shown by curve 2 in Fig. 1(a).

the solitonic part of the radiation field remains well-localized in the form of a short light pulse, the remaining part of the field spreading out over a few picoseconds.

To visualize the significance of the Raman effect, we compare in Figs. 3(a) and 3(b) the evolution of a few-cycle laser pulse in a PCF simulated with and without the Raman term in Eq. (1). This comparison shows that, when the Raman effect is artificially switched off, the redshifting of radiation beyond the spectral band centered at 920 nm is arrested. The output spectra are then dominated by the features related to SPM and FWM (the spectral bands centered at 670 and 920 nm). No soliton-fission dynamics, considered in earlier work on supercontinuum generation in PCFs [14], is expected in this case since the input field energy is sufficient to produce only the fundamental soliton in the fiber, which is clearly seen as a well-resolved peak in the time domain [the insets in Figs. 3(a) and 3(b)]. The missing redshifted solitonic part of the spectrum makes a striking difference between the results of simulations performed without the Raman term in Eq. (1) and the experimentally observed PCF output, presented and discussed in the following section of this paper.

III. EXPERIMENTAL

Experimental studies of nonlinear-optical transformations of few-cycle pulses in two types of PCFs with the above-specified parameters were performed with a broadband chirped-mirror Ti:sapphire oscillator [28], generating 6-fs pulses with an energy up to 4 nJ at a repetition rate of 70 MHz. The laser output was divided into two channels of roughly equal energies with a beamsplitter. One of the resulting beams was reserved for pumping a Nd:YAG (yttrium-

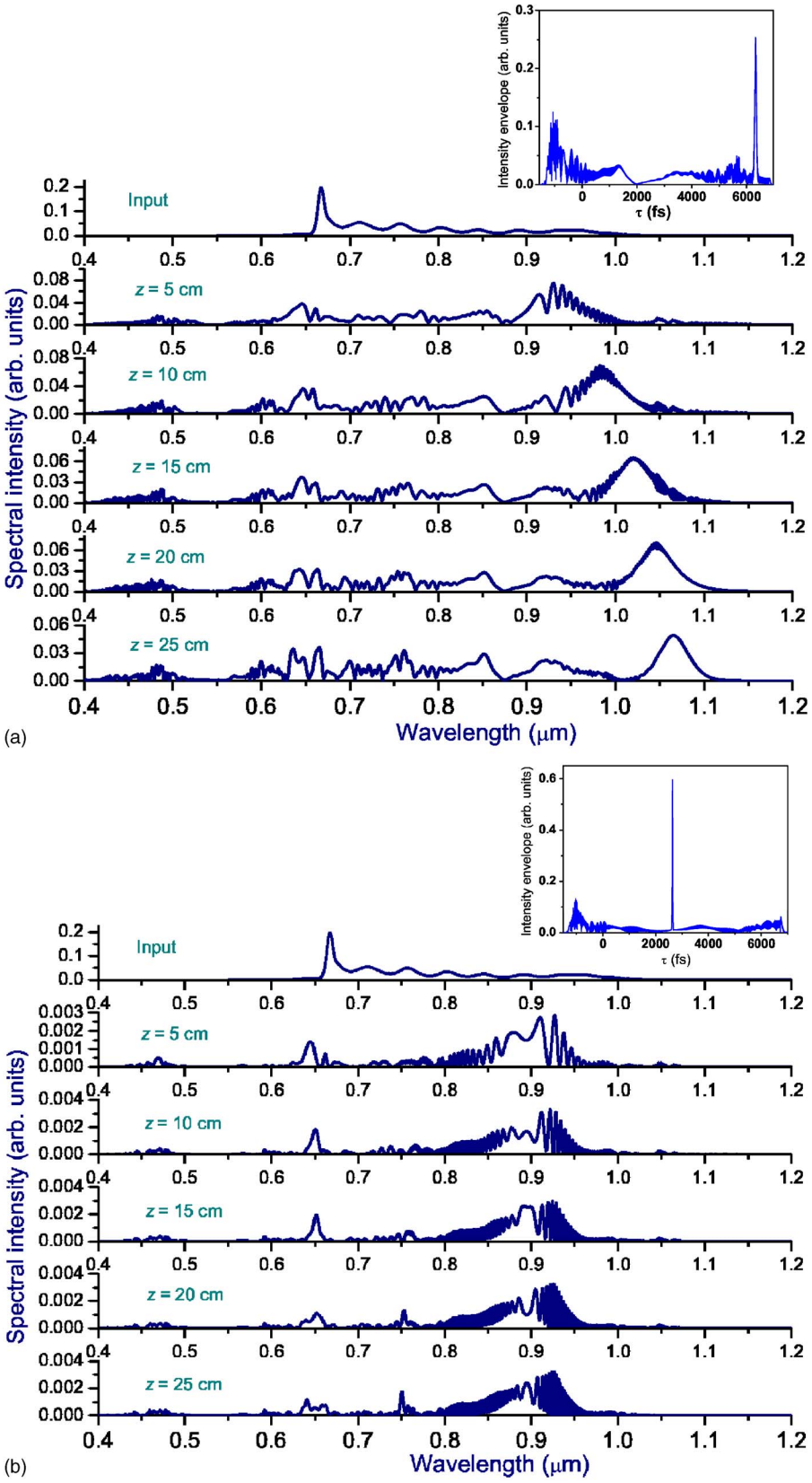

FIG. 3. (Color online) Spectral evolution of a laser pulse with an initial energy of 0.3 nJ and an input temporal envelope and chirp shown in Fig. 1(b) propagating through the PCF with the dispersion profile as shown by curve 1 in Fig. 1(a) (a) with and (b) without the Raman term in the generalized nonlinear Schrödinger equation. The insets show the time-domain structure of the radiation field in the PCF for $z = 25$ cm (a) with and (b) without the Raman effect.

aluminum-garnet) regenerative amplifier [29], while the second beam was sent into the PCF, providing, with allowance for fiber-coupling losses, initial pulse energies in the nano- to subnanojoule range.

In Figs. 4(a) and 4(b), we present intensity spectra measured at the output of the NL-PM-750 fiber and a PCF with a cross-section structure shown in the inset to Fig. 1(a). The spectrum, chirp, and temporal envelope of the input pulse are

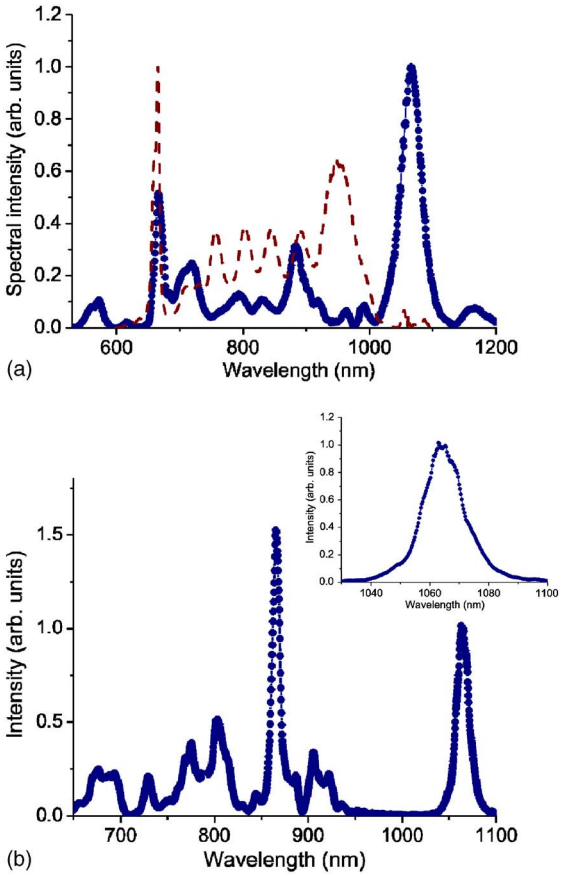

FIG. 4. (Color online) Filled circles connected with a solid line show experimental spectra measured at the output of (a) a 20-cm NL-PM-750 fiber and (b) a 23-cm PCF with a cross-section structure shown in the inset to Fig. 1(a). The dashed line in (a) presents the input spectrum, provided by the Ti:sapphire oscillator. The inset in (b) shows the close-up of the 1064-nm soliton peak in the output of the PCF output spectrum.

specified by Figs. 1(a) and 1(b). Both output spectra presented in Figs. 4(a) and 4(b) feature a spectrally isolated peak centered at approximately 1060 nm, as predicted by numerical simulations [cf. Figs. 2(b) and 4(a)]. This signal is shifted by more than 180 THz with respect to the maximum-intensity peak at 670 nm in the spectrum of the input laser pulse. An interference filter with a base length of 1.1 μm was used to study this spectral component in greater detail. The result of this investigation is presented in the inset to Fig. 4(b). The energy of the spectrally selected 1060-nm output of the PCF was estimated as 10 pJ. With the total radiation energy at the output of the fiber being about 0.3 nJ, the efficiency of energy conversion to the redshifted soliton peak at 1060 nm is estimated as 3%. The contrast of this signal, defined as the ratio of spectral intensities at 1060 and 1025 nm, exceeds 200.

Our theoretical model, as can be seen from the comparison of theoretical and experimental PCF output spectra presented in Figs. 2(b) and 4(a), gives interesting physical insights into the dominant spectral features in PCF output. Based on the results of our simulations in Fig. 2(b), we identify the peaks at 550 and 1060 nm in Fig. 4(a) as the signatures of Cherenkov emission of dispersive waves and the redshifted soliton, respectively. The prominent peaks at 670 and 890 nm in Fig. 4(a) are indicative of phase-matched FWM processes around the zero-GVD wavelength, which give rise, as shown in Fig. 2(b), to two characteristic peaks at 670 nm and around 900 nm and deplete the pulse spectrum between these wavelengths. On the other hand, simulations for the spectral evolution of a short pulse without the Raman term in Eq. (1) show [Fig. 3(b)] that FWM in our experiments does not transfer the radiation energy beyond 900–950 nm. Energy conversion to the redshifted peaks at 1060 nm in Figs. 4(a) and 4(b) is therefore indicative of Raman-induced soliton self-frequency shift.

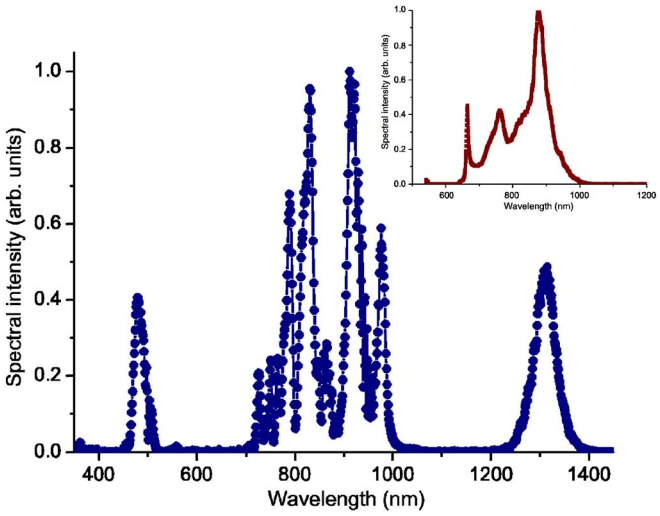

FIG. 5. (Color online) Spectrum of radiation intensity at the output of a 20-cm NL-PM-750 fiber with a modified spectrum of the input ultrashort laser pulse (shown in the inset).

In Fig. 5, we present the results of experiments where the spectrum of the input pulse has been changed by replacing the mirrors in the Ti:sapphire oscillator. The pulse duration remains about 6 fs, but the spectral content of the input field is now different (see the inset in Fig. 5), with a higher spectral intensity provided within the range of wavelengths from 750 to 950 nm. This change in the input spectrum does not lead to qualitative changes in the spectrum at the output of the PCF, which still features signatures of self-phase modulation and four-wave mixing in the central part of the spectrum and well-resolved peaks corresponding to a redshifted soliton and Cherenkov emission of dispersive waves (Fig. 5). An input field with more energy concentrated in the near-infrared part of the spectrum, as can be seen from the comparison of Figs. 4 and 5, allows the generation of redshifted solitons with longer central wavelengths. With the fiber parameters (dispersion profile and the fiber length) remaining the same as in Fig. 4(a), the frequency-shifted soliton is now observed as an isolated peak centered at 1310 nm in the output spectrum [Fig. 5(a)]. This finding demonstrates the possibility of controlling the central wavelength of redshifted solitons at the output of PCFs by modifying the spectrum of the input pulse.

IV. CONCLUSION

We have shown in this work that photonic-crystal fibers can provide a high efficiency of spectral transformation of few-cycle laser pulses. With the wavelength of zero group-velocity dispersion of the fiber lying within the broad spectrum of the input pulse, the output spectra observed in our experiments are dominated by distinct spectral peaks, originating from concurrent nonlinear-optical processes. We have identified well-resolved signatures of soliton self-frequency shift, four-wave mixing, and Cherenkov emission of dispersive waves and demonstrate that the laser pulse energy can be efficiently coupled into a spectrally isolated redshifted peak centered at 1060 nm. This spectral peak can carry up to 3% of radiation energy at the output of the fiber and is ideally suited as a seed for Nd:YAG- and ytterbium-based laser devices. Generation of intense redshifted soliton peaks centered at 1310 nm has been demonstrated by increasing the energy concentrated in the near-infrared part of the spectrum of the input few-cycle laser pulse.

ACKNOWLEDGMENTS

We are grateful to K.V. Dukel'skii, A.V. Khokhlov, Yu.N. Kondrat'ev, and V.S. Shevandin for fabricating fiber samples. E.E.S. and A.M.Z. acknowledge partial support of their research by the Russian Foundation for Basic Research (Projects No. 03-02-16929, No. 04-02-81036-Bel2004, No. 04-02-39002-GFEN2004, and No. 03-02-20002-BNTS-a), INTAS (Projects No. 03-51-5037 and No. 03-51-5288), and the Federal Program of Russian Federation on microstructure fiber components. The research described in this publication was made possible in part by Award No. RP2-2558 of the U.S. Civilian Research & Development Foundation for the Independent States of the Former Soviet Union (CRDF). This work was also supported by Laserlab Europe and XTRA EU networks. A.B. and C.Y.T. acknowledge partial support of their research by the German Research Foundation (DFG).

[1] *Few-Cycle Laser Pulse Generation and Its Applications*, edited by F. X. Kärtner (Springer, Berlin, 2004).
[2] T. Brabec and F. Krausz, Rev. Mod. Phys. **72**, 545 (2000).
[3] P. St. J. Russell, Science **299**, 358 (2003).
[4] J. C. Knight, Nature (London) **424**, 847 (2003).
[5] W. J. Wadsworth, A. Ortigosa-Blanch, J. C. Knight, T. A. Birks, T. P. M. Mann, and P. St. J. Russell, J. Opt. Soc. Am. B **19**, 2148 (2002).
[6] D. A. Akimov, E. E. Serebryannikov, A. M. Zheltikov, M. Schmitt, R. Maksimenka, W. Kiefer, K. V. Dukel'skii, V. S. Shevandin, and Yu. N. Kondrat'ev, Opt. Lett. **28**, 1948 (2003).
[7] W. H. Reeves, D. V. Skryabin, F. Biancalana, J. C. Knight, P. St. J. Russell, F. G. Omenetto, A. Efimov, and A. J. Taylor, Nature (London) **424**, 511 (2003).
[8] J. K. Ranka, R. S. Windeler, and A. J. Stentz, Opt. Lett. **25**, 25 (2000).
[9] *Supercontinuum Generation*, Special issue of Appl. Phys. B: Lasers Opt. **77** (2/3) (2003), edited by A. M. Zheltikov.
[10] A. B. Fedotov, A. M. Zheltikov, A. P. Tarasevitch, and D. von der Linde, Appl. Phys. B: Lasers Opt. **73**, 181 (2001).
[11] J. M. Dudley, L. Provino, N. Grossard, H. Maillotte, R. S. Windeler, B. J. Eggleton, and S. Coen, J. Opt. Soc. Am. B **19**, 765 (2002).
[12] St. Coen, A. H. L. Chau, R. Leonhardt, J. D. Harvey, J. C. Knight, W. J. Wadsworth, and Ph. St. J. Russell, Opt. Lett. **26**, 1356 (2001).
[13] S. Coen, A. H. L. Chau, R. Leonhardt, J. D. Harvey, J. C. Knight, W. J. Wadsworth, and P. St. J. Russell, J. Opt. Soc. Am. B **19**, 753 (2002).
[14] J. Herrmann, U. Griebner, N. Zhavornokov, A. Husakou, D. Nickel, J. C. Knight, W. J. Wadsworth, P. St. J. Russell, and G. Korn, Phys. Rev. Lett. **88**, 173901 (2002).
[15] D. V. Skryabin, F. Luan, J. C. Knight, and P. St. J. Russell, Science **301**, 1705 (2003).
[16] X. Liu, C. Xu, W. H. Knox, J. K. Chandalia, B. J. Eggleton, S. G. Kosinski, and R. S. Windeler, Opt. Lett. **26**, 358 (2001).
[17] A. N. Naumov, A. B. Fedotov, A. M. Zheltikov, V. V. Yakovlev, L. A. Mel'nikov, V. I. Beloglazov, N. B. Skibina, and A. V. Shcherbakov, J. Opt. Soc. Am. B **19**, 2183 (2002).
[18] G. Genty, M. Lehtonen, and H. Ludvigsen, Opt. Express **12**, 4614 (2004).
[19] B. R. Washburn, S. E. Ralph, and R. S. Windeler, Opt. Express **10**, 575 (2002).
[20] G. P. Agrawal, *Nonlinear Fiber Optics* (Academic, San Diego, 2001).
[21] K. J. Blow and D. Wood, IEEE J. Quantum Electron. **25**, 2665 (1989).
[22] T. M. Monro, D. J. Richardson, N. G. R. Broderick, and P. J. Bennet, J. Lightwave Technol. **18**, 50 (2000).
[23] http://www.crystal-fibre.com/
[24] F. M. Mitschke and L. F. Mollenauer, Opt. Lett. **11**, 659 (1986).
[25] E. M. Dianov, A. Ya. Karasik, P. V. Mamyshev, A. M. Prokhorov, V. N. Serkin, M. F. Stel'makh, and A. A. Fomichev, JETP Lett. **41**, 294 (1985).
[26] P. K. A. Wai, H. H. Chen, and Y. C. Lee, Phys. Rev. A **41**, 426 (1990).
[27] N. Akhmediev and M. Karlsson, Phys. Rev. A **51**, 2602 (1995).
[28] T. Fuji, A. Unterhuber, V. S. Yakovlev, G. Tempea, A. Stingl, F. Krausz, and W. Drexler, Appl. Phys. B: Lasers Opt. **77**, 125 (2003).
[29] C. Y. Teisset, N. Ishii, T. Fuji, T. Metzger, S. Köhler, R. Holzwarth, A. Baltuška, A. M. Zheltikov, and F. Krausz, Opt. Express **13**, 6550 (2005).